Supplementary information

Boosting activity toward oxygen reduction reaction of a mesoporous FeCuNC catalyst via heteroatom doping-induced electronic state modulation

Jong Gyeong Kim[a], Jinwon Cho[b], Seung Soon Jang[b], Hyejin Lee[c], Eunsung Yuk[c,d], Byungchan Bae[c,d], Sunghoon Han[a], Chanho Pak[a*]

[a]*Graduate School of Energy Convergence, Institute of Integrated Technology, Gwangju Institute of Science and Technology, Gwangju 61005, Republic of Korea*

[b]*School of Materials Science and Engineering, Georgia Institute of Technology, Atlanta GA 30332-0245, United States*

[c]*Fuel Cell Laboratory, Korea Institute of Energy Research, Daejeon 34129, South Korea*

[d]*Renewable Energy Engineering, Korea University of Science and Technology (UST), 217, Gajeong-ro, Yuseong-gu, Daejeon 34113, South Korea*

[*]**Corresponding author.** Email: chanho.pak@gist.ac.kr, tel.: +82-62-715-5324

Table S1. Specific surface area, micro-, meso-, and total pore volume of $FeCu_{0.5}NC$, $FeCu_{1.0}NC$, and $FeCu_{1.5}NC$.

	S_{BET}[a] (m^2/g)	V_{micro}[b] (cm^3/g)	V_{meso}[c] (cm^3/g)	V_p[d] (cm^3/g)
$FeCu_{0.5}NC$	950	0.21	0.70	0.91
$FeCu_{1.0}NC$	910	0.18	0.76	0.94
$FeCu_{1.5}NC$	900	0.21	0.60	0.81

a: Specific surface area; b: Micropore volume; c: Mesopore volume; d: Total pore volume

Table S2. Composition of FeNC, $FeCu_{1.0}NC$, and CuNC from ICP-OES, EA, and XPS survey.

	ICP (wt.%)			**EA (wt.%)**			**XPS (at%)**		
	Fe	Cu	C	N	S	C	N	P	S
FeNC	2.9	-	78.1	4.1	-	94.8	2.19	0.09	-
$FeCu_{1.0}NC$	3.2	2.5	77.1	4.2	0.5	94.5	2.21	0.08	0.17
CuNC	-	2.7	71.1	3.9	0.4	95.9	2.17	0.14	0.15

Table S3. Composition of N species in FeNC, $FeCu_{1.0}NC$, and CuNC.

at%	Pyridinic N	M-N	Pyrrolic N	Graphitic N	Oxidized N
FeNC	29.8	10.6	6.5	40.4	12.7
$FeCu_{1.0}NC$	30.0	11.7	7.4	41.1	9.8
CuNC	29.2	10.0	5.9	40.7	14.2

Table S4. EXAFS fitting parameters of FeNC, $FeCu_{1.0}NC$, and CuNC.

Sample	Path	*N*	*R* (Å)	σ^2 (Å^2)	ΔE_0 (eV)	*R*, %	R range	k range
FeNC	Fe-N	3.10	2.03	0.007	2.91	0.1 (0.001)	1.0 – 2.4 Å	2.0 – 8.0 Å
	Fe-C1	1.09	2.05	0.002				
	Fe-C2	3.73	2.63	0.015				
$FeCu_{1.0}NC$_Fe	Fe-N	3.09	1.98	0.013	-0.02	0.8 (0.008)	0.9 – 2.0 Å	2.5 – 9.4 Å
	Fe-C	1.17	2.01	0.008				
$FeCu_{1.0}NC$_Cu	Cu-N	2.90	1.85	0.002	-11.98	0.9 (0.009)	1.0 – 2.0 Å	2.1 – 10.5 Å
	Cu-C	1.04	1.86	0.002				
CuNC	Cu-N	2.94	1.91	0.005	-9.79	0.4 (0.004)	1.0 – 2.0 Å	2.5 – 9.7 Å
	Cu-C	1.05	1.95	0.003				

- Amplitude reduction factor (SO^2): Fe (0.78); Cu (0.86)

Table S5. Comparison of H_2/O_2 AEMFC and PGM-free cathodes based on previously reported literature.

Cathode catalyst	Catalyst loading (mg/cm^2)		Membrane	Current density (A/cm^2) @0.6 V	Peak power density (W/cm^2)	Operating temperature (^oC)
	Cathode (NPMC)	Anode (PGM)				
$FeCu_{1.0}NC$ (This study)	2.2	0.7	FAA-3-50	0.49	0.294	70
CF-VC[1]	2.4	0.7	LDPE	1.45	1.35	70
FeCoPc/C[2]	0.3	1.0	LDPE	1.61	1.26	80
Fe-N-Gra[3]	2.0	0.8	HMT-PMBI	0.34	0.243	60
CoFe-N-CDC/CNT[4]	0.75	0.74	ETFE	1.69	1.12	60
Fe-N-CDC/CNT[4]	0.71	0.74	ETFE	1.13	1.06	60
N-C-CoO_x[5]	2.4	0.7	LDPE-BTMA	1.32	1.05	65
Fe/N/CNT[6]	2.0	0.4	aQAPS-S_8	0.47	0.49	60
Pyrolysed KB/FePc[7]	2.0	0.8	HMT-PMBI	0.22	0.186	60
FePc/C[8]	1	0.4	Tokuyama A901	0.19	0.120	55
$Fe_{0.5}$-NH_3[9]	0.9	0.6	HDPE	1.78	1.4	65
New Fe-N-C[10]	1	0.125	HDPE	1.70	1.3	80
New Fe-N-C[10]	1	0.6	HDPE	2.72	2.05	80

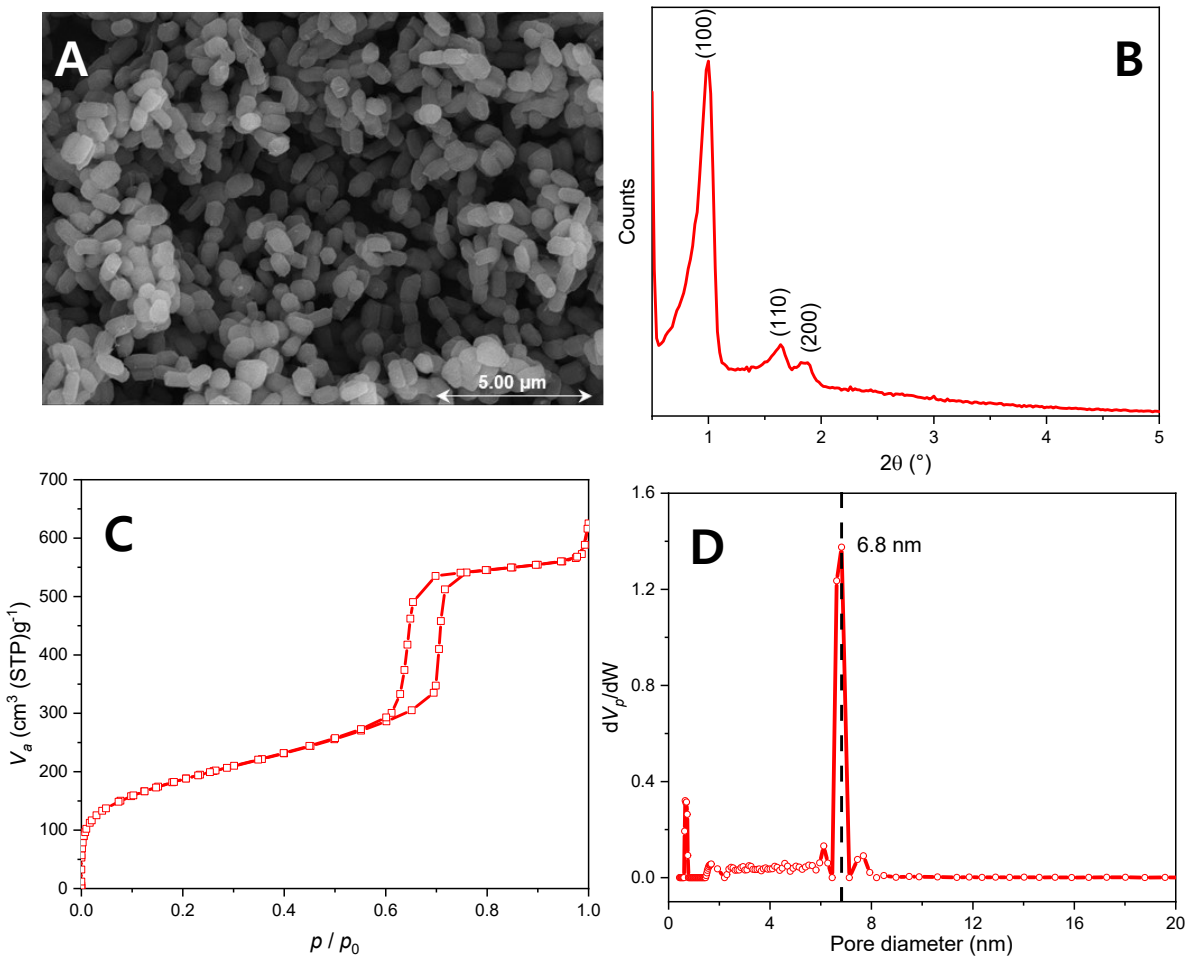

Figure S1. SEM image (A), XRD pattern (B), N_2 adsorption isotherm, and pore size distribution of grain-shaped SBA-15.

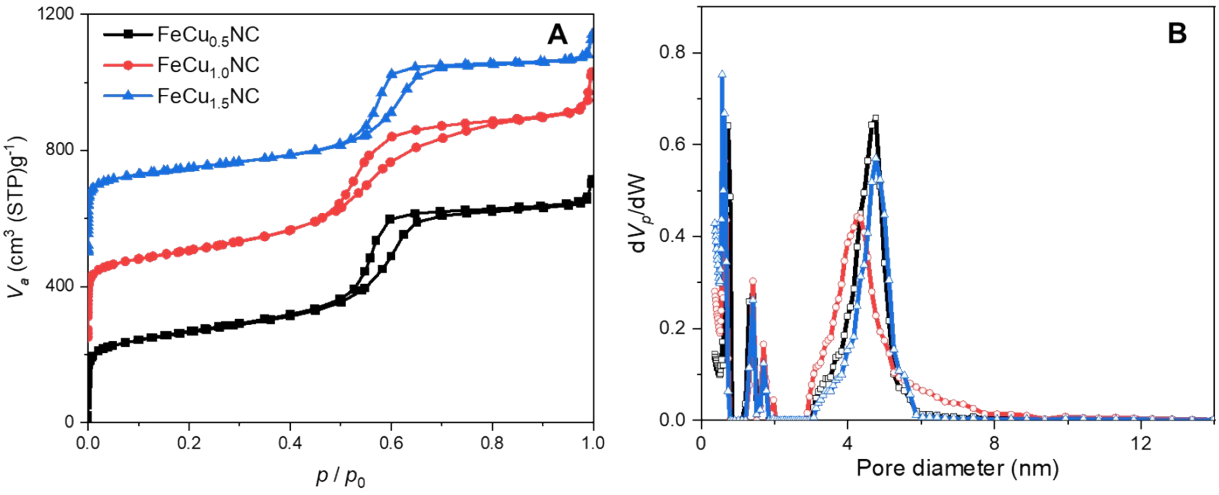

Figure S2. N_2 adsorption curves (A) and pore size distributions (B) of $FeCu_{0.5}NC$, $FeCu_{1.0}NC$, and $FeCu_{1.5}NC$.

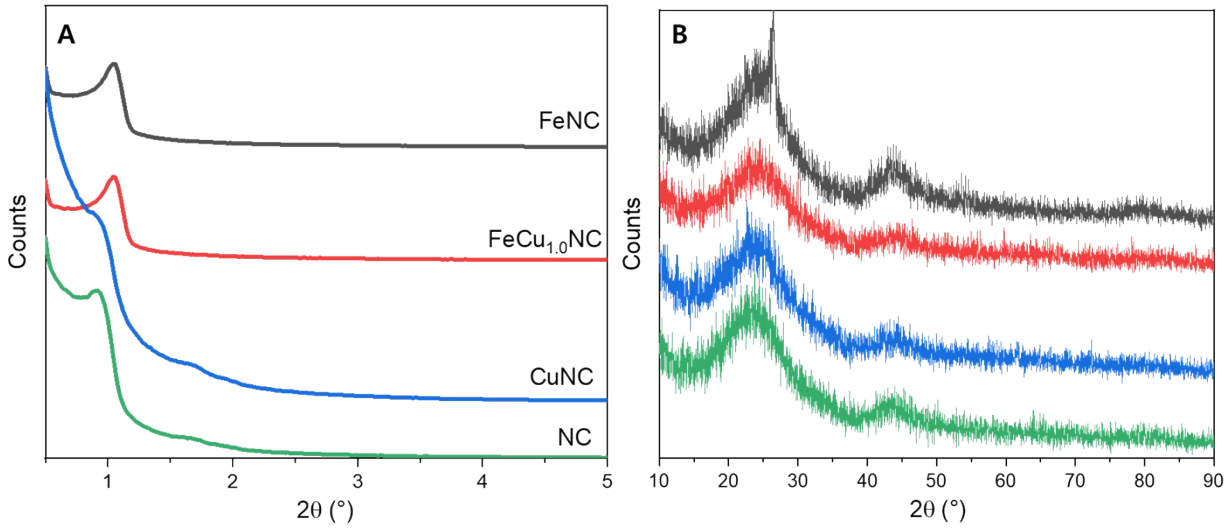

Figure S3. X-ray patterns at low-angle range (0.5–5°) (A) and mid-angle range (10–90°) (B) of FeNC, $FeCu_{1.0}NC$, CuNC, and NC.

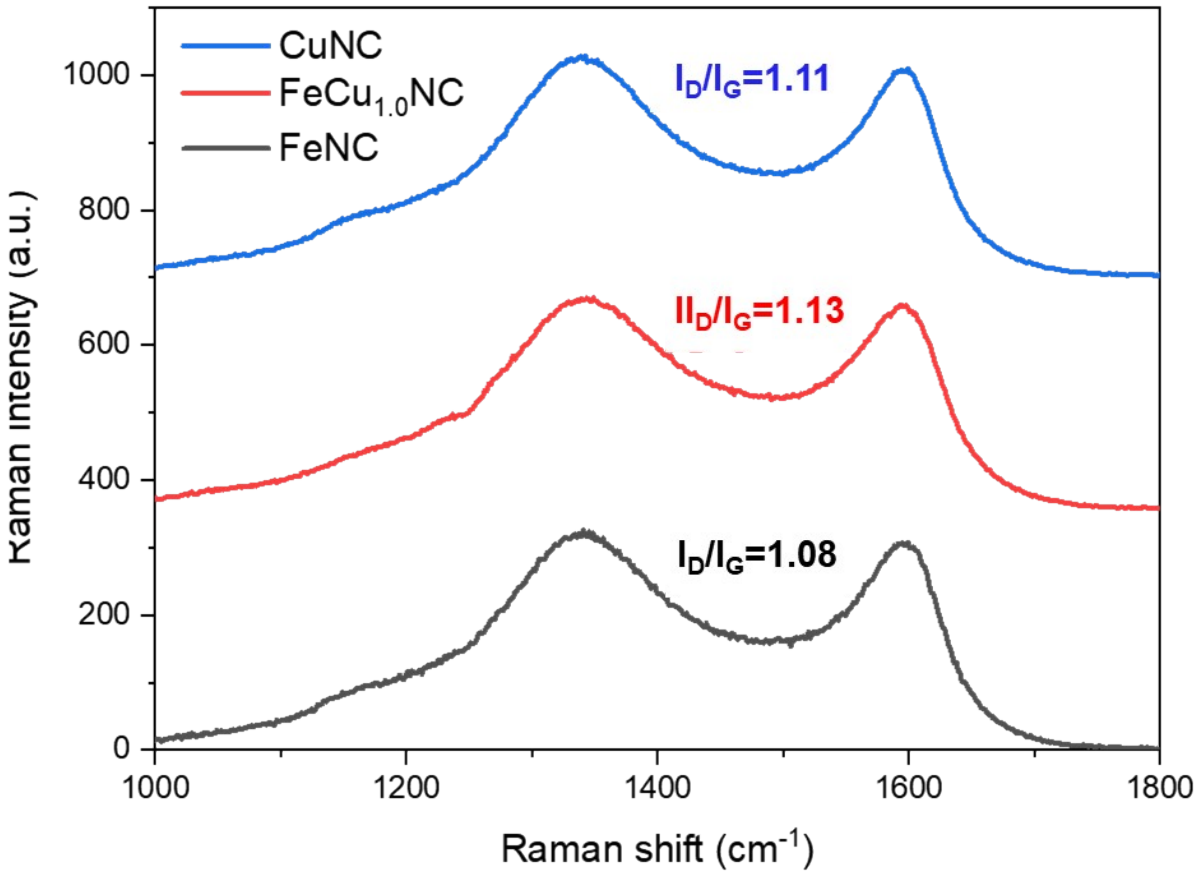

Figure S4. Raman spectra of FeNC, $FeCu_{1.0}NC$, and CuNC.

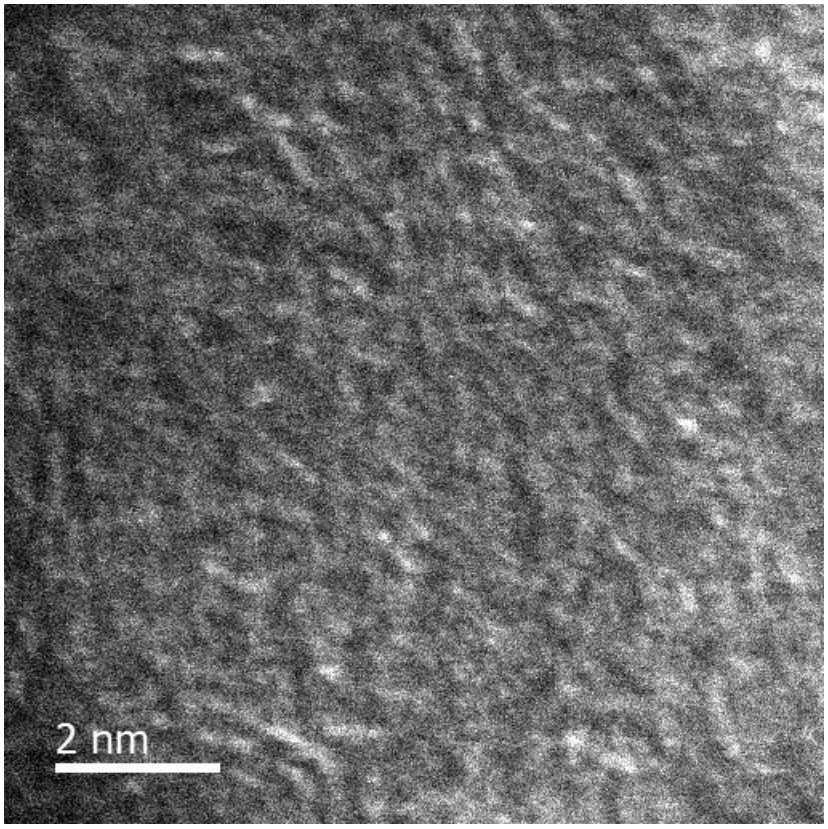

Figure S5. HAADF-STEM image of FeNC at atomic resolution.

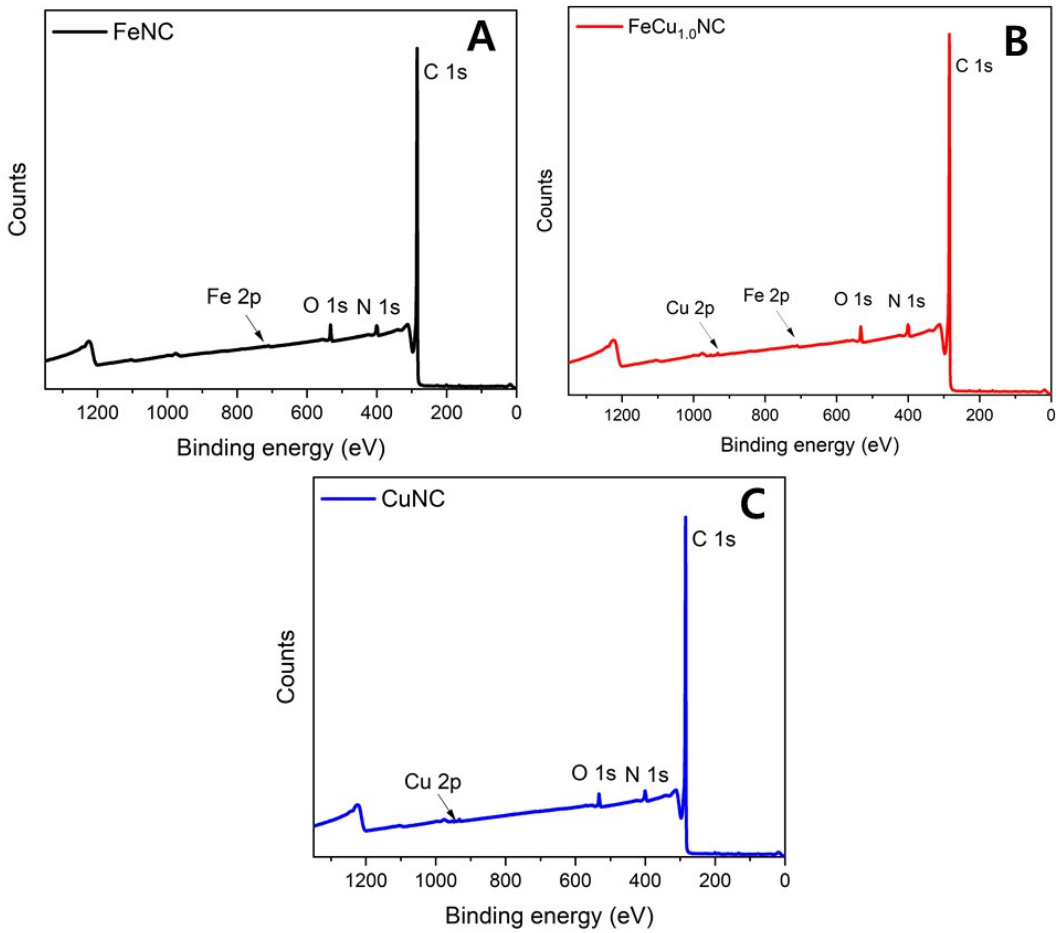

Figure S6. XPS survey of FeNC (A), $FeCu_{1.0}NC$ (B), CuNC (C).

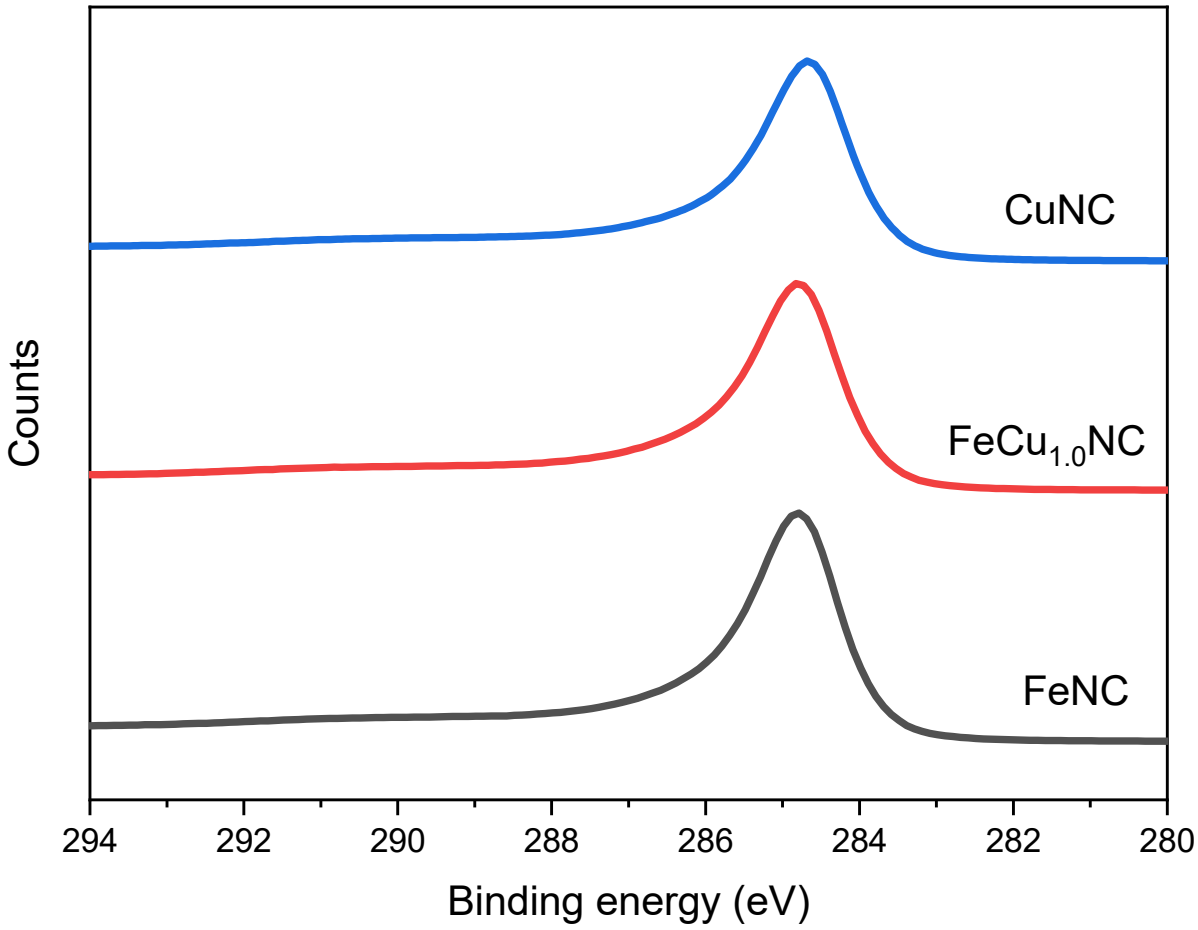

Figure S7. C1s spectra of FeNC, $FeCu_{1.0}NC$, CuNC.

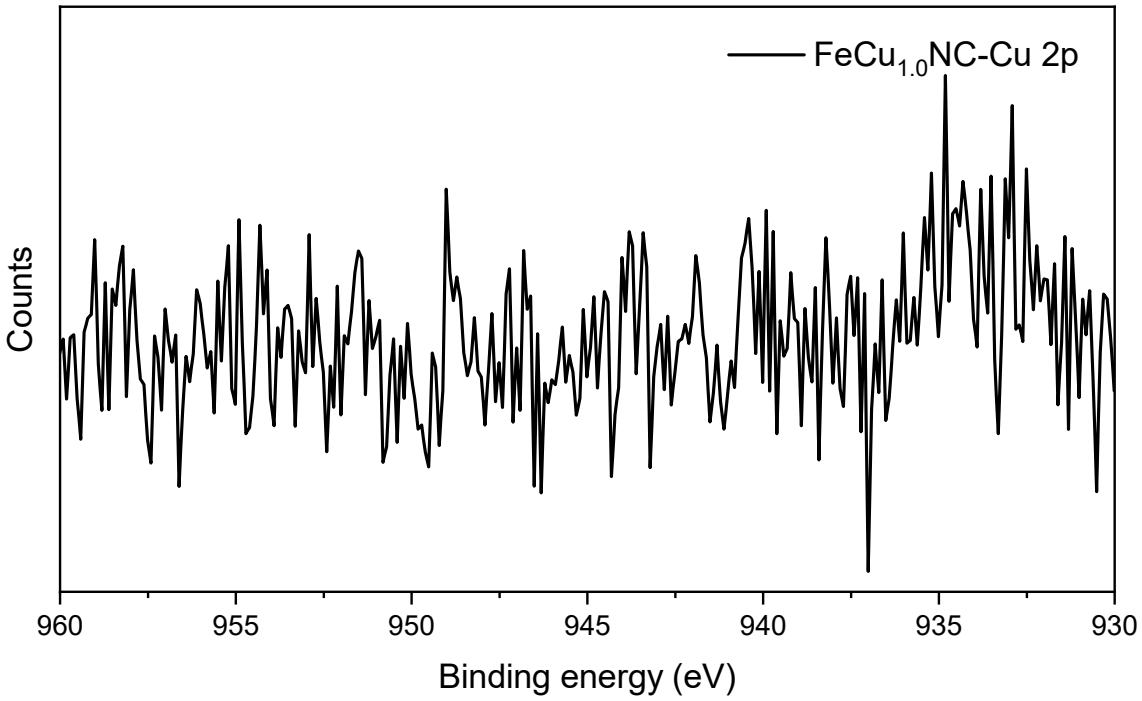

Figure S8. Cu 2p spectrum of $FeCu_{1.0}NC$.

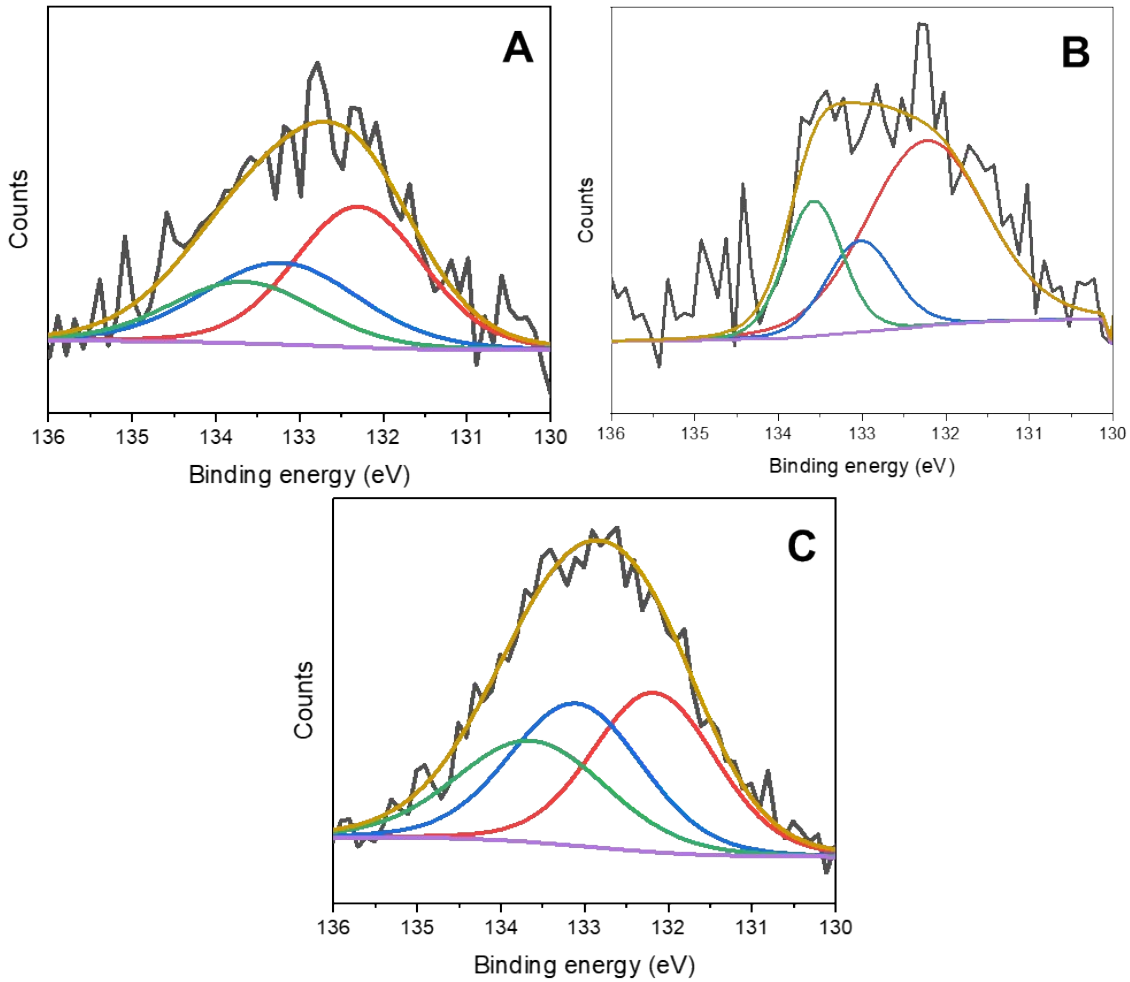

Figure S9. P 2p spectra of FeNC (A), $FeCu_{1.0}NC$ (B), CuNC (C).

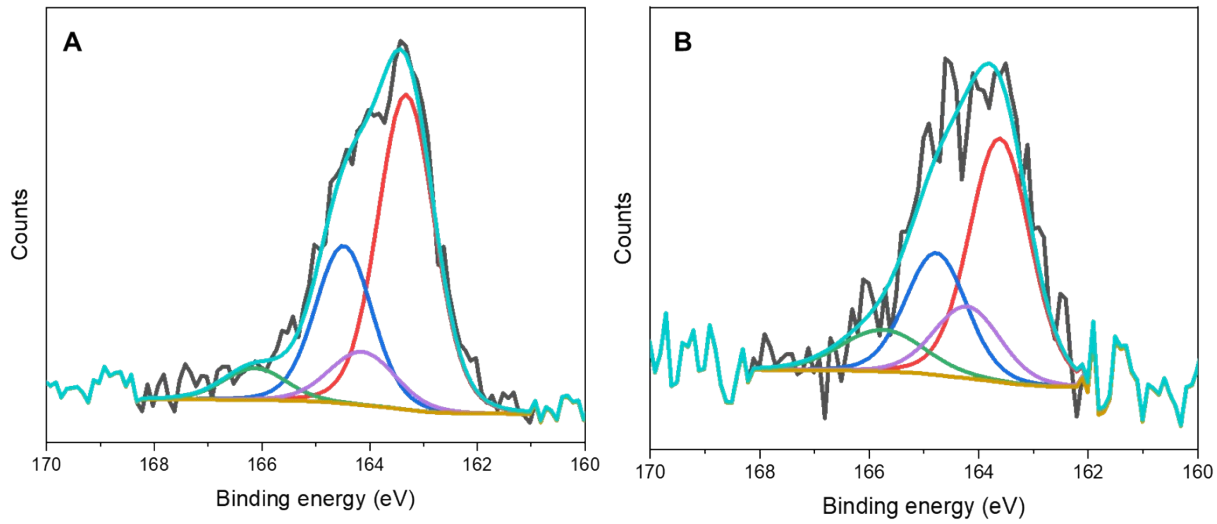

Figure S10. S 2p spectra of $FeCu_{1.0}NC$ (A), CuNC (B).

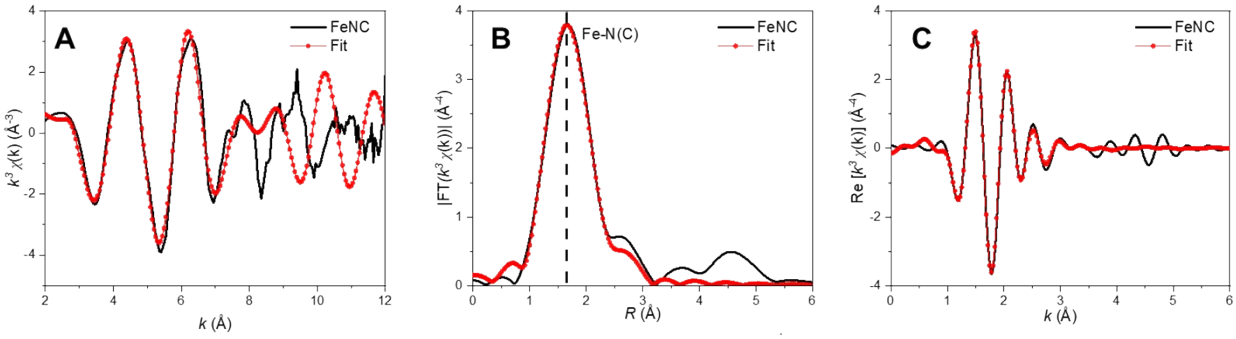

Figure S11. Raw data and their fit in *k* space (A), $R_{magnitude}$ (B), and R_{real} (C) part of FeNC in the Fe K-edge.

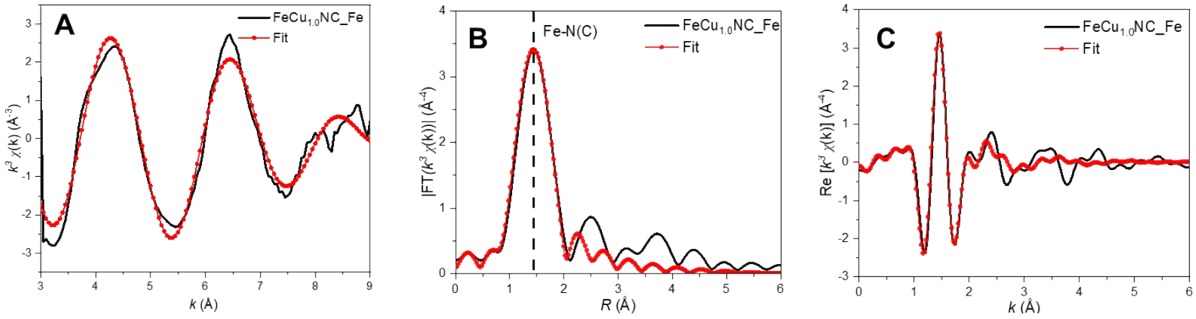

Figure S12. Raw data and their fit in *k* space (A), $R_{magnitude}$ (B), and R_{real} (C) part of FeCuNC in the Fe K-edge.

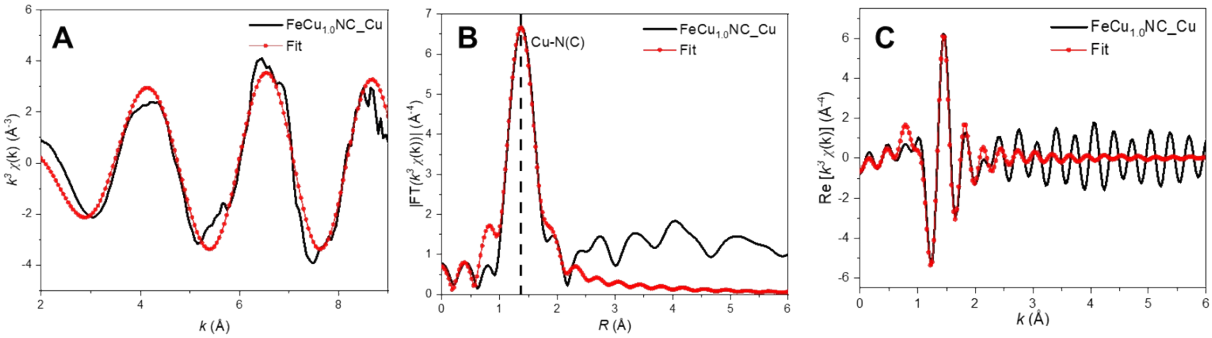

Figure S13. Raw data and its fit in *k* space (A), $R_{magnitude}$ (B), and R_{real} (C) part of $FeCu_{1.0}NC$ in the Cu K-edge.

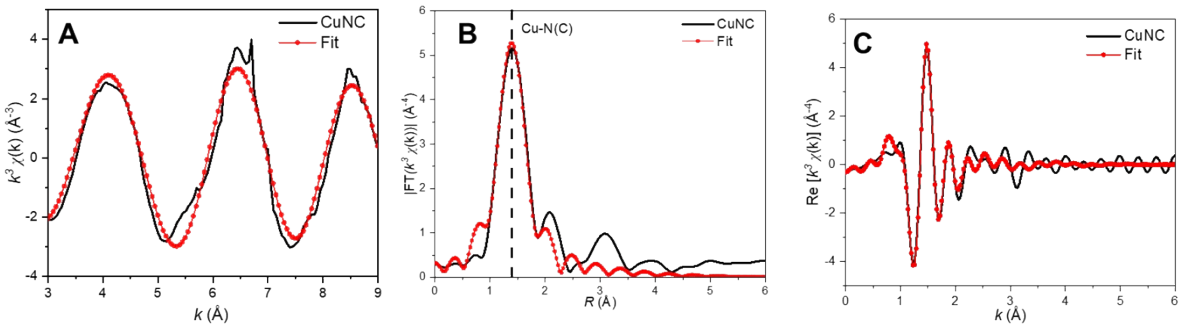

Figure S14. Raw data and its fit in *k* space (A), $R_{magnitude}$ (B), and R_{real} (C) part of CuNC in the Cu K-edge.

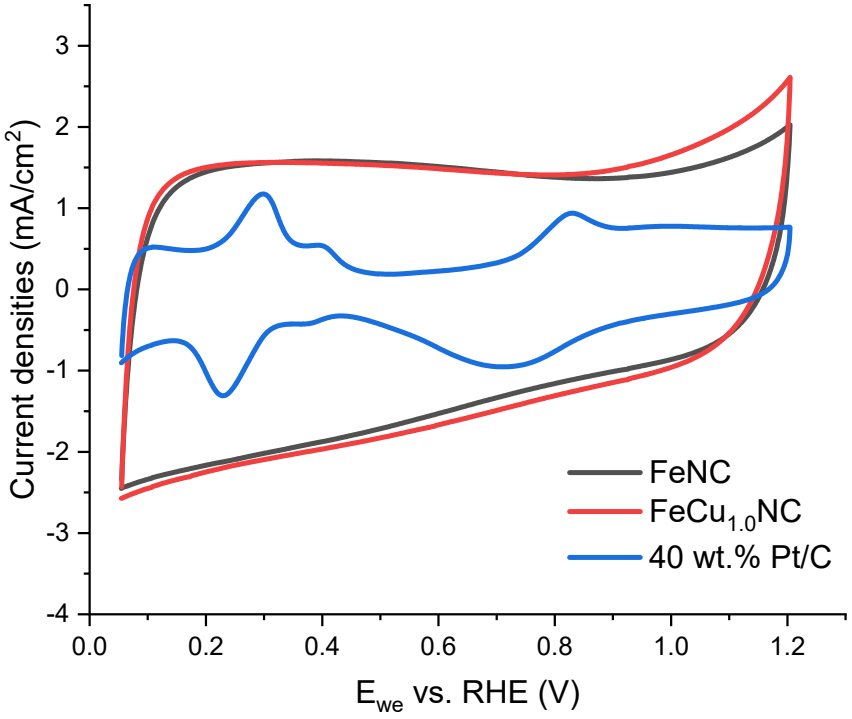

Figure S15. Cyclic voltammograms of FeNC, $FeCu_{1.0}NC$, and 40 wt.% Pt/C in 0.1 M KOH.

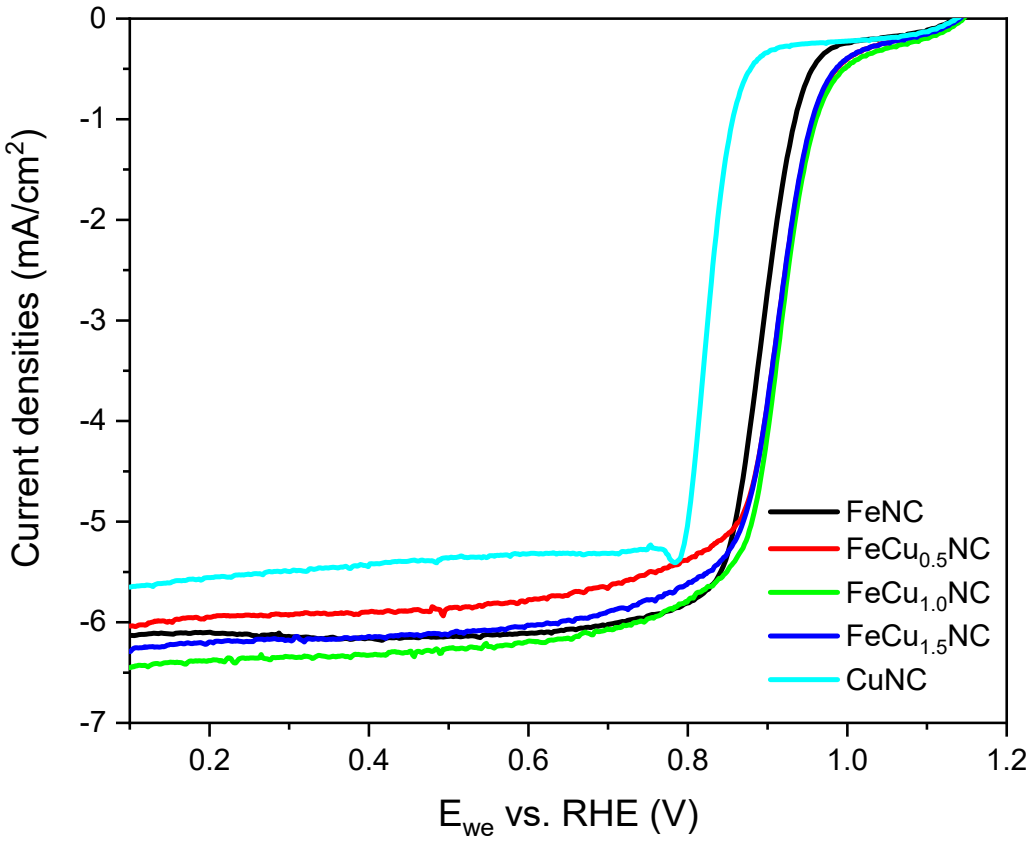

Figure S16. Linear sweep voltammogram of FeNC, $FeCu_{0.5}NC$, $FeCu_{1.0}NC$, $FeCu_{1.5}NC$, and CuNC in 0.1 M KOH at 10 mV/s.

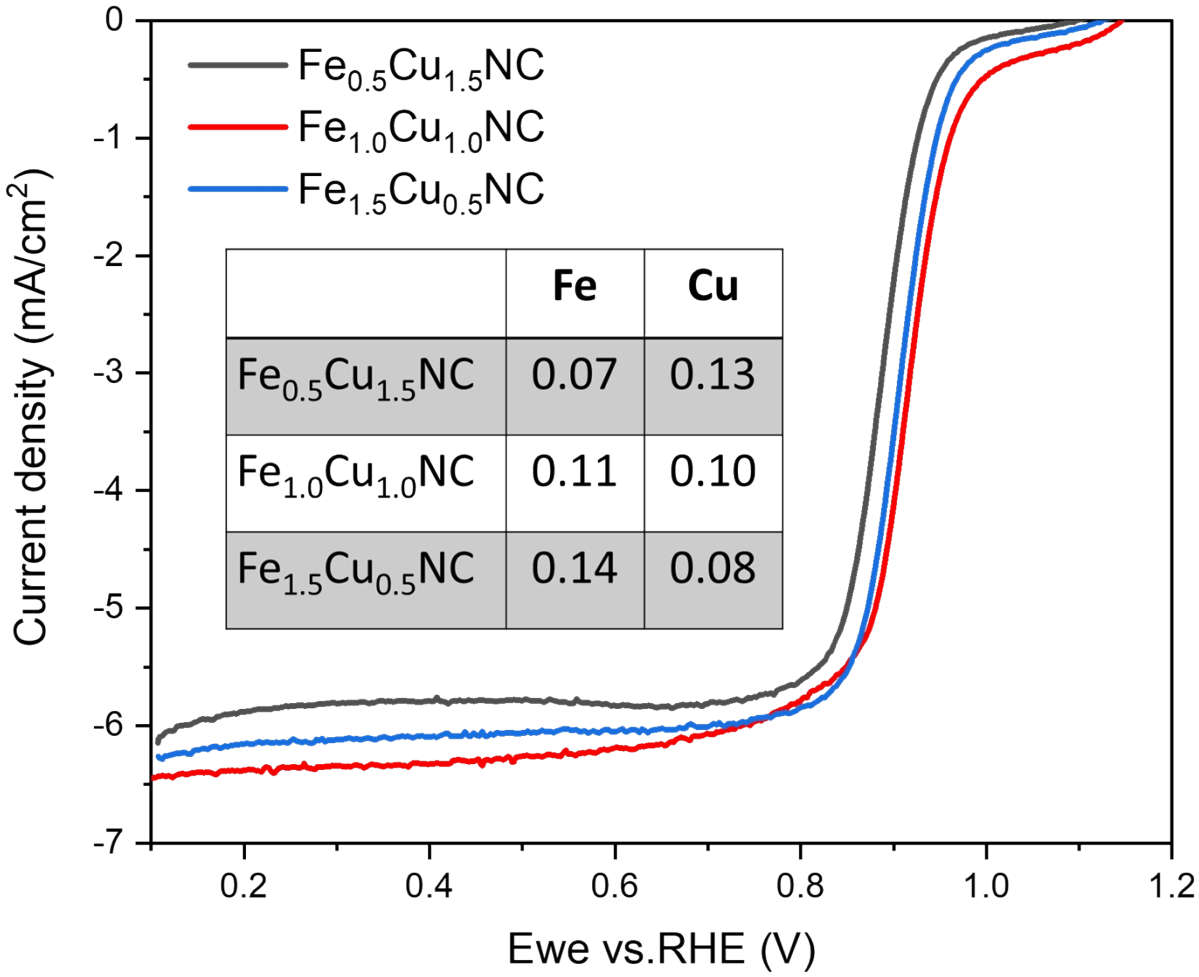

	Fe	Cu
$Fe_{0.5}Cu_{1.5}NC$	0.07	0.13
$Fe_{1.0}Cu_{1.0}NC$	0.11	0.10
$Fe_{1.5}Cu_{0.5}NC$	0.14	0.08

Figure S17. Linear sweep voltammogram of FeCuNC catalysts with different Fe to Cu atomic ratio in 0.1 M KOH at 10 mV/s. Inset table is amount of Fe and Cu (at%) measured from XPS.

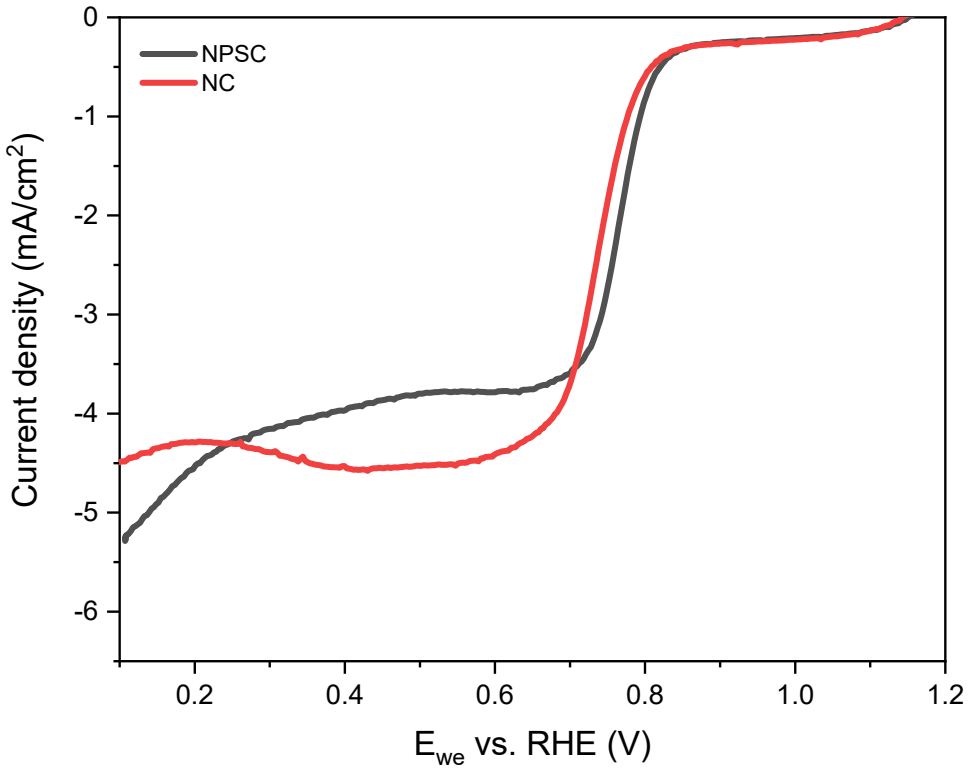

Figure S18. Linear sweep voltammogram of NC and NPSC in 0.1 M KOH at 10 mV/s.

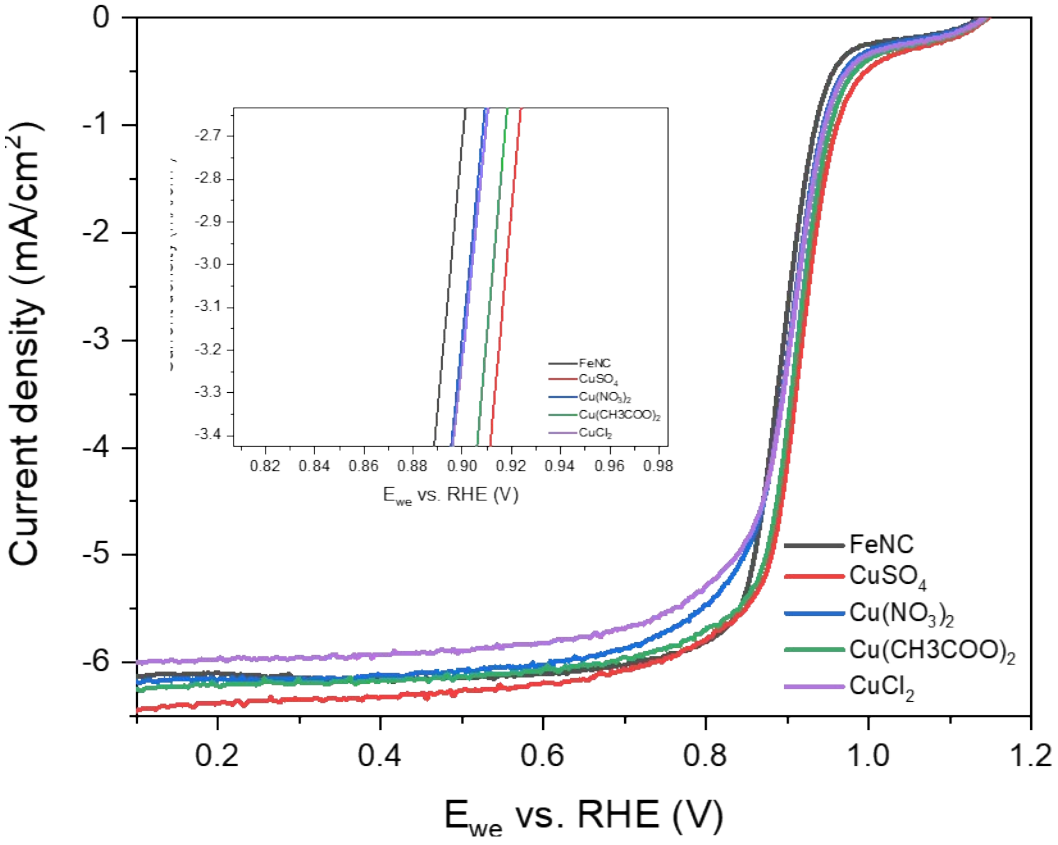

Figure S19. Linear sweep voltammogram of FeCuNC catalysts with different Cu precursors in 0.1 M KOH at 10 mV/s

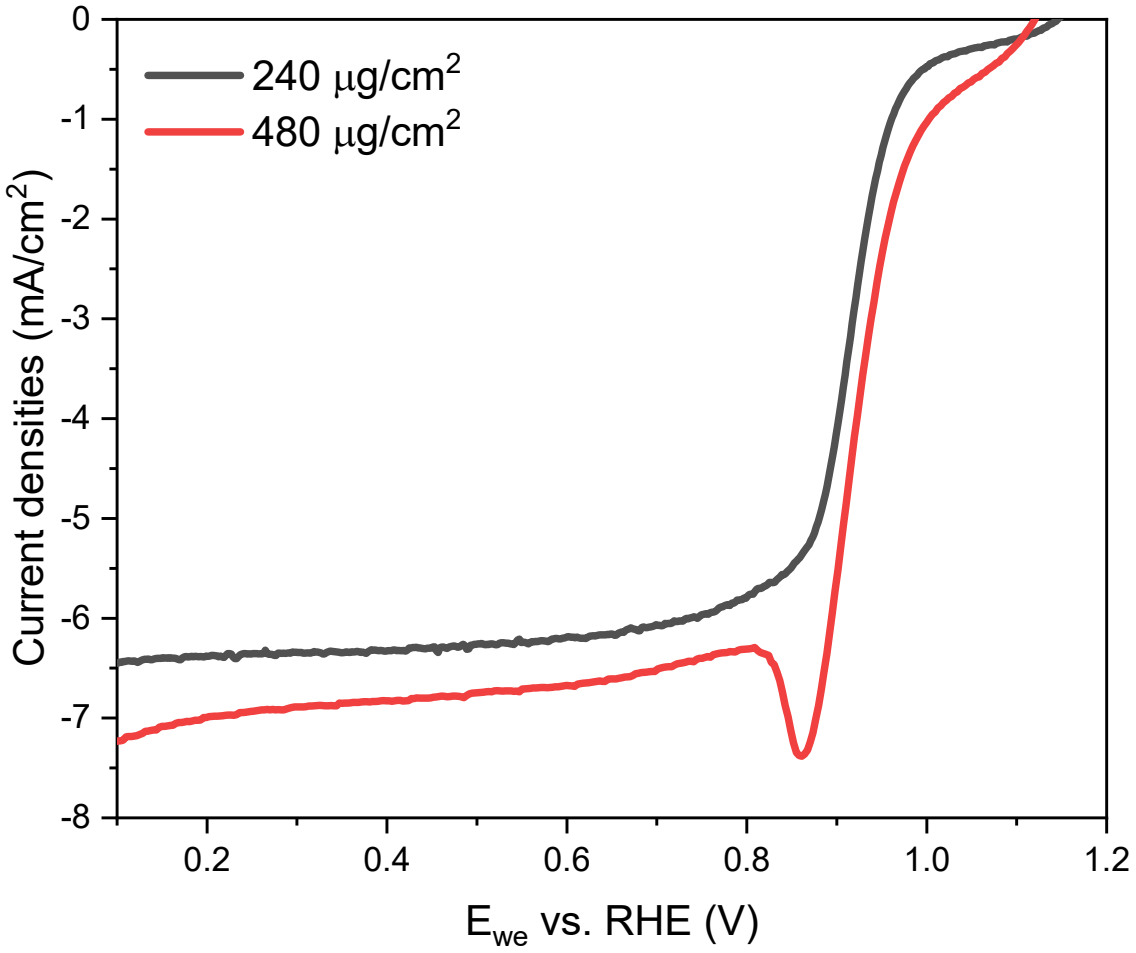

Figure S20. Linear sweep voltammogram of $FeCu_{1.0}NC$ with different loading amounts on a glassy carbon working electrode in 0.1 M KOH at 10 mV/s.

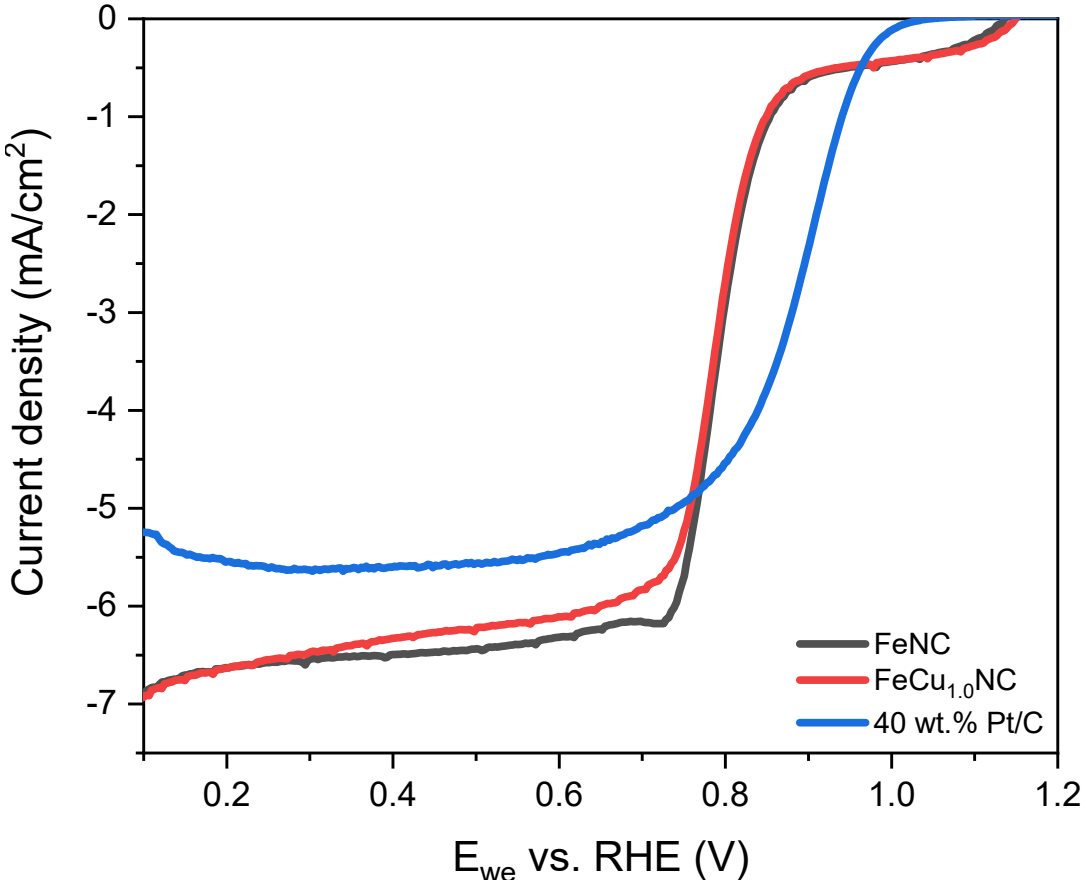

Figure S21. Linear sweep voltammogram of FeNC, $FeCu_{1.0}NC$, and Pt/C in 0.1 M $HClO_4$ at 10 mV/s.

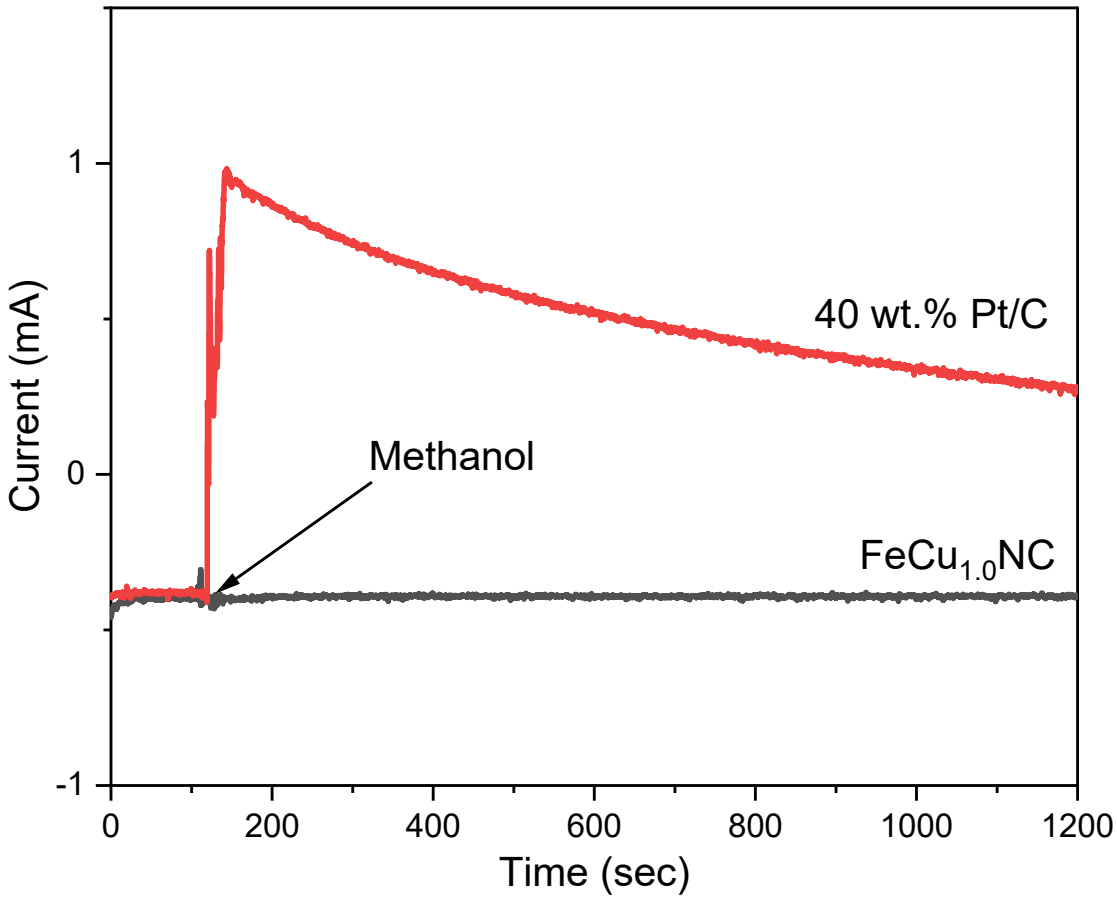

Figure S22. Methanol resistance of Pt/C and $FeCu_{1.0}NC$.

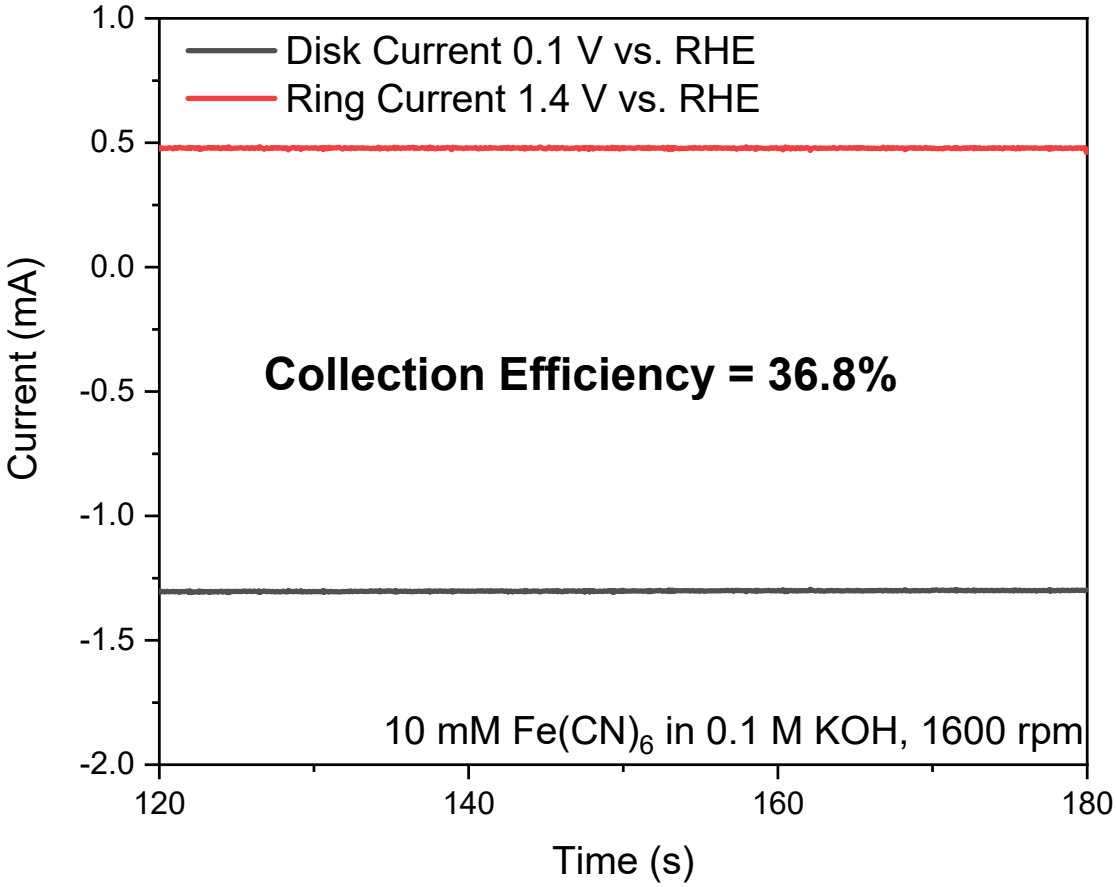

Figure S23. Result of collection efficiency experiment for $FeCu_{1.0}NC$. Collection efficiency was calculated by averaging current densities in the last 60 s.

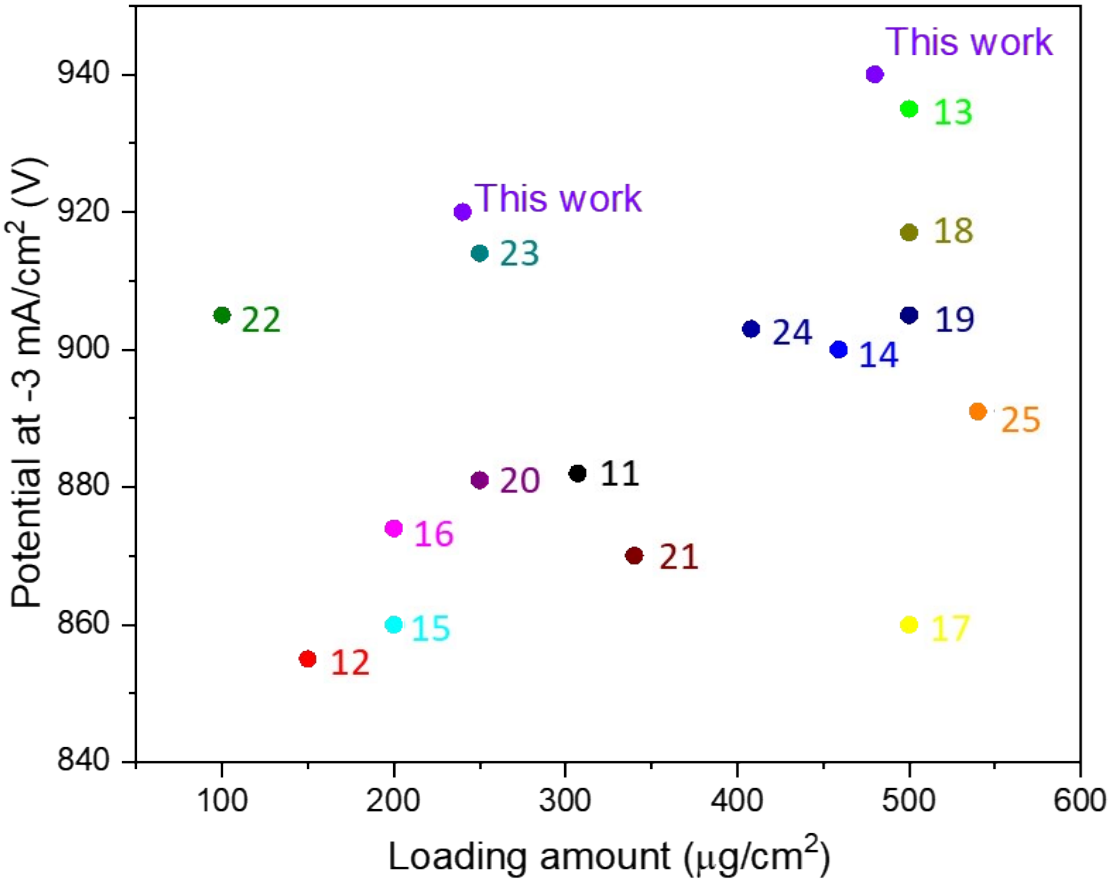

Figure S24. Comparison of the ORR (0.1 M KOH) catalytic activities (potential at -3 mA/cm^2) determined in previous studies.

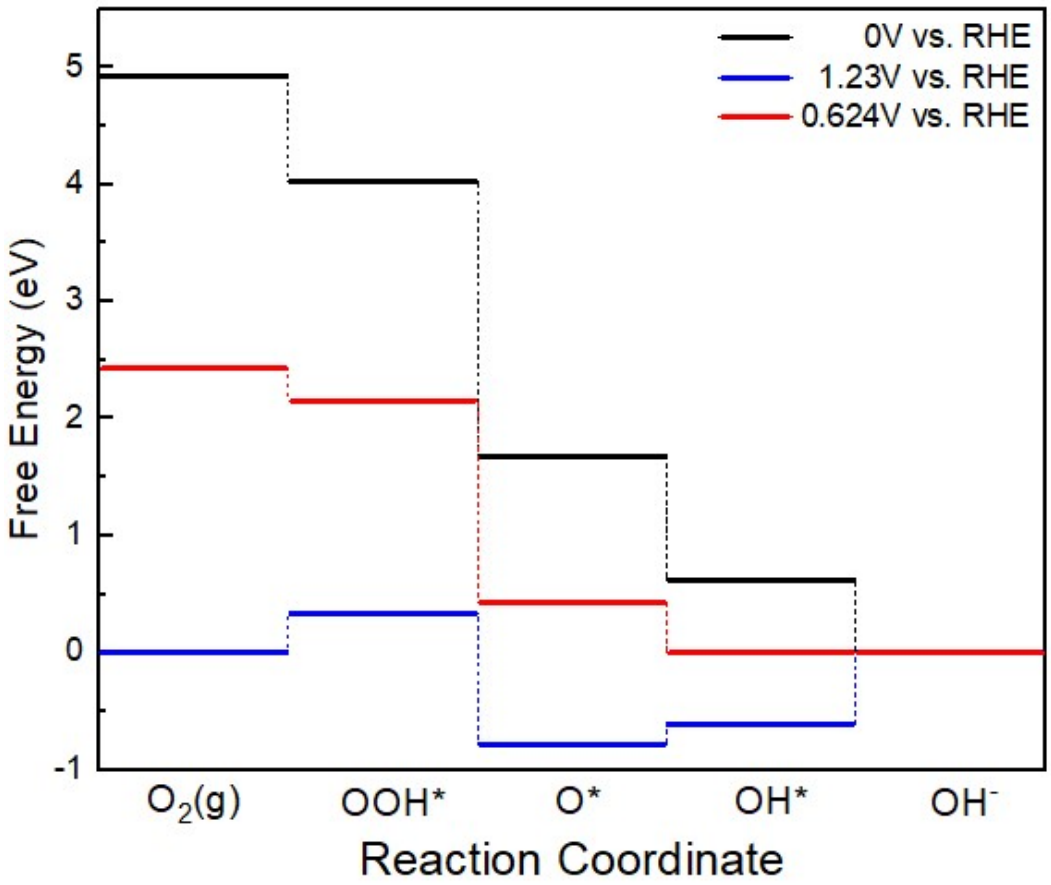

Figure S25. Calculated potential energy diagram at various applied potentials U for Fe-N_3-C-P-S model, such as open circuit voltage (0 V), equilibrium potential (1.23 V), and onset potential versus RHE, which is displayed in black, blue, and red bars, respectively.

References

1. X. Peng, V. Kashyap, B. Ng, S. Kurungot, L. Wang, J. Varcoe and W. Mustain, *Catalysts*, 2019, **9**, 264.

2. L. Wang, M. Bellini, H. A. Miller and J. R. Varcoe, *J. Mater. Chem. A*, 2018, **6**, 15404–15412.

3. R. Sibul, E. Kibena-Põldsepp, S. Ratso, M. Kook, M. T. Sougrati, M. Käärik, M. Merisalu, J. Aruväli, P. Paiste, A. Treshchalov, J. Leis, V. Kisand, V. Sammelselg, S. Holdcroft, F. Jaouen and K. Tammeveski, *ChemElectroChem*, 2020, **7**, 1739–1747.

4. J. Lilloja, E. Kibena-Põldsepp, A. Sarapuu, J. C. Douglin, M. Käärik, J. Kozlova, P. Paiste, A. Kikas, J. Aruväli, J. Leis, V. Sammelselg, D. R. Dekel and K. Tammeveski, *ACS Catal.*, 2021, **11**, 1920–1931.

5. X. Peng, T. J. Omasta, E. Magliocca, L. Wang, J. R. Varcoe and W. E. Mustain, *Angew. Chem. Int. Ed.*, 2018, **131**, 1058–1063.

6. H. Ren, Y. Wang, Y. Yang, X. Tang, Y. Peng, H. Peng, L. Xiao, J. Lu, H. D. Abruña and L. Zhuang, *ACS Catal.*, 2017, **7**, 6485–6492.

7. R. Praats, M. Käärik, A. Kikas, V. Kisand, J. Aruväli, P. Paiste, M. Merisalu, J. Leis, V. Sammelselg, J. H. Zagal, S. Holdcroft, N. Nakashima and K. Tammeveski, *Electrochim. Acta*, 2020, **334**, 135575.

8. H. A. Miller, M. Bellini, W. Oberhauser, X. Deng, H. Chen, Q. He, M. Passaponti, M. Innocenti, R. Yang, F. Sun, Z. Jiang and F. Vizza, *Phys. Chem. Chem. Phys.*, 2016, **18**, 33142–33151.

9. H. A. Firouzjaie and W. E. Mustain, *ACS Catal.*, 2019, **10**, 225–234.

10. H. Adabi, A. Shakouri, N. Ul Hassan, J. R. Varcoe, B. Zulevi, A. Serov, J. R. Regalbuto and W. E. Mustain, *Nat. Energy*, 2021, **6**, 834–843.

11. Z. Xiao, Y. Wu, S. Cao, W. Yan, B. Chen, T. Xing, Z. Li, X. Lu, Y. Chen, K. Wang and J. Jiang, *Chem. Eng. J.*, 2021, **413**, 127395.

12. J. Lee, H. S. Kim, J.-H. Jang, E.-H. Lee, H.-W. Jeong, K.-S. Lee, P. Kim and S. J. Yoo, *ACS Sustain. Chem. Eng.*, 2021, **9**, 7863-7872.

13. Y.-M. Zhao, P.-C. Zhang, C. Xu, X.-Y. Zhou, L.-M. Liao, P.-J. Wei, E. Liu, H. Chen, Q. He and J.-G. Liu, *ACS Appl. Mater. Interfaces*, 2020, **12**, 17334-17342.

14. D. Wang, H. Xu, P. Yang, X. Lu, J. Ma, R. Li, L. Xiao, J. Zhang and M. An, *J. Mater. Chem. A*, 2021, **9**, 13678-13687.

15. X. Cui, L. Gao, S. Lei, S. Liang, J. Zhang, C. D. Sewell, W. Xue, Q. Liu, Z. Lin and Y. Yang, *Adv. Funct. Mater.*, 2021, **31**, 2009197.

16. X. Liang, Z. Li, H. Xiao, T. Zhang, P. Xu, H. Zhang, Q. Gao and L. Zheng, *Chem. Mater.*, 2021, **33**, 5542-5554.

17. L. Zheng, S. Yu, X. Lu, W. Fan, B. Chi, Y. Ye, X. Shi, J. Zeng, X. Li, and S. Liao, *ACS Appl. Mater. Interfaces*, 2020, **12**, 13878-13887.

18. J. Deng, S. Chen, Q. Zhou, Y. Nie, J. Li, R. Wu, Q. Wang and Z. Wei, *J. Power Sources*, 2020, **451**, 227808.

19. S. Yin, G. Li, X. Qu, J. Zhang, L. Shen, Y. Li, C. Wang, Z. Yu, B. Lu, B. Xu, Y. Jiang and S. Sun, *ACS Appl. Energy Mater.*, 2020, **3**, 625-634.

20. Y. Ha, B. Fei, X. Yan, H. Xu, Z. Chen, L. Shi, M. Fu, W. Xu and R. Wu, *Adv. Energy Mater.*, 2020, **10,** 2002592.

21. W. Gu, M. Wu, J. Sun, J. Xu and T. Zhao, *J. Mater. Chem. A*, 2019, **7**, 20132-20138.

22. W. Cheng, P. Yuan, Z. Lv, Y. Guo, Y. Qiao, X. Xue, X. Liu, W. Bai, K. Wang, Q. Xu and J. Zhang, *Appl. Catal., B*, 2020, **260**, 118198.

23. Z. Yang, Y. Wang, M. Zhu, Z. Li, W. Chen, W. Wei, T. Yuan, Y. Qu, Q. Xu, C. Zhao, X. Wang, P. Li, Y. Li, Y. Wu and Y. Li, *ACS Catal.*, 2019, **9**, 2158-2163.

24. Y. Chen, S. Ji, Y. Wang, J. Dong, W. Chen, Z. Li, R. Shen, L. Zheng, Z. Zhuang, D. Wang and Y. Li, *Angew. Chem., Int. Ed.*, 2017, **56**, 6937-6941.

25. F. Xiao, G.L. Xu, C.J. Sun, M. Xu, W. Wen, Q. Wang, M. Gu, S. Zhu, Y. Li, Z. Wei, X. Pan, J. Wang, K. Amine and M. Shao, *Nano Energy*, 2019, **61**, 60-68.